Anal. Bioanal. Electrochem., Vol. 16, No. 9, 2024, 862-880
https://www.doi.org/10.22034/abec.2024.716172

Analytical & Bioanalytical Electrochemistry

Full Paper

Corrosion Protection Performance of a Derivative of Quinoline [5-((3-Propyl-1H-Pyrrol-1-Yl) Methyl) Quinolin-8-Ol] PPMQ On Carbon Steel in Hydrochloric Acidic Solution 1 M

Chadine Belmejdoub,[1,2,*] Khalid Benbouya,[1] Issam Forsal,[2] Sara Lahmady,[2] Mohamed Rbaa,[3] and Rachid Touir[4]

[1]*EMDD_CERNE2D, Mohamed V University of Rabat, EST Salé, Morocco*
[2]*Laboratory of Engineering and Applied Technologies, School of Technology, Beni Mellal, Morocco*
[3]*Laboratory of Organic Chemistry, Catalysis and Environment, Faculty of Sciences, Ibn Tofail University, PO Box 133, 14000, Kenitra, Morocco*
[4]*Regional Center for Education and Training Professions (CRMEF), Kenitra, Morocco*

*Corresponding Author, Tel.: +212661118208
E-Mail: belmejdoubchadine@gmail,com

Received: 25 February 2024 / Received in revised form: 2 September 2024 / Accepted: 10 September 2024 / Published online: 30 September 2024

Abstract- Organic inhibitors play a crucial role in the corrosion inhibition process. In this work, the performance of the derivative of quinoline PPMQ against corrosion of carbon steel in the acidic medium HCl 1 M was assessed using electrochemical methods. The findings of the experiments showed that the inhibitor had a strong inhibitory impact on the metal tested in the hydrochloric acid solution. The outcomes of the study displayed that the inhibition efficiency of the tested inhibitor enhanced with its concentrations and remained almost stable during immersion time while decreasing slightly with rising temperature. Electrochemical measurements of this study showed that the corrosion was greatly decreased by the organic inhibitor through a charge transfer mechanism with a high inhibition efficiency of 95.58% at an optimal concentration of 10^{-2} M at 293 K. While potentiodynamic polarization data reported that the inhibitor was a mixed-type inhibitor. PPMQ was inclined towards the Langmuir adsorption isotherm by spontaneous chemical-physical adsorption on the surface of carbon steel. Additionally, thermodynamic and activation data revealed that this action occurs through an endothermic process. Scanning electron microscopy findings showed that the inhibitor's molecules form a protective layer, which confirms the electrochemical results.

Keywords- Organic inhibitor; Acidic medium; Electrochemical measurements; SEM analysis; Thermodynamic parameters

1. INTRODUCTION

In the present day, carbon steel is widely utilized in several industries, including the petroleum industry, infrastructure maintenance, and metal coating applications, due to its robust mechanical and physical properties. Still, this metal alloy, when surrounded by an acidic environment, once subjected to different processes like acidization that is widely used as an effective method in these industries, can deteriorate due to corrosion [1,2].

Inhibitors are of paramount importance in the prevention of corrosion. Typically, they are incorporated into the acid solution, to prevent damage and mitigate corrosion on carbon steel surfaces [2]. These inhibitors are chemicals designed to minimize or prevent corrosion by creating a layer of protection on the steel's surface that prohibits the acid from reaching the metal. This makes them an effective and commonly employed method for examining how corrosion inhibition affects carbon steel in acidic media [3]. Corrosion inhibitors are specifically designed to mitigate the corrosive effects of acids on metals and can provide valuable insights into the effectiveness of various inhibitors and their performance in real-world conditions.

Organic inhibitors are frequently composed of heteroatoms, including nitrogen (N), oxygen (O), sulfur (S), and aromatic ring molecules, as well as groups that are polar with π-electrons. Which makes these chemical features significant in preventing corrosion. Among these molecules comes quinoline and its derivatives, which are commonly employed as anticorrosive compounds due to their ability to effectively inhibit metallic corrosion [4].

Several recent reports have highlighted the application of quinoline-based products in inhibiting corrosion. These studies have explored synthesizing and evaluating different quinoline derivatives with polar substituents for corrosion inhibition applications.

In fact, it has been found that quinoline derivatives that possess polar functional groups at the 8th position, including 8-hydroxyquinoline (8-HQ), 8-methoxyquinoline (8-MQ), 8-aminoquinoline (8-AQ), and 8-nitroquinoline (8-NQ), among others, form chelating complexes with metal surfaces that exhibit a high degree of stability [5-7].

According to numerous studies, these compounds play a significant role as ingredients of pharmacologically active synthetic compounds [8]. They exhibit many biological activities, including robust DNA binding capacities [9], anticancer effects [10], and the ability to serve as DNA-intercalating carriers [11]. Among these drugs, the compound 5-((3-propyl-1H-pyrrol-1-yl) methyl) quinoline-8-ol with the chemical formula $C_{17}H_{18}N_2O$**,** serves as an antibacterial agent.

Lakhrissi et al. have worked on the antibacterial activity of this drug and revealed that it remained active in low concentrations against three Gram-positive and Gram-negative bacterial strains (E. coli, S. aureus and P. aeruginosa) [12].

The aim of our work, is to examine the compound 5-((3-propyl-1H-pyrrol-1-yl) methyl) quinoline-8-ol for its impact as an organic inhibitor on the behavior of carbon steel in 1M hydrochloric acid solution. Let's refer to the inhibitor substance as PPMQ.

The concentration of PPMQ utilized in the experiments varied from 10^{-5} M to 10^{-2} M. We analyzed the corrosion behavior of carbon steel by studying the effects of PPMQ concentration, the environment temperature (from 293 K to 323 K), and immersion time (ranging from 0.5 hours to 14 hours). The corrosion processes were assessed using electrochemical techniques, including potentiodynamic polarization and electrochemical spectroscopy impedance. Additionally, thermodynamic parameters associated with PPMQ adsorption on the surface of the carbon steel were estimated and discussed to understand the inhibitory properties of PPMQ.

2. EXPERIMENTAL SECTION

2.1. Material

The experiments conducted involved the use of carbon steel with the chemical composition as follows: (wt.%): C~0.07, Mn~0.19, Si~0.03, Cr~0.05, Al~0.02, and the remainder iron (Fe). This composition indicates the weight percentages of different elements present in the carbon steel. The carbon steel specimen dimensions being (0.9 cm×0.9cm) have been used for experimental purposes.

To prepare the aggressive solution, 1 M hydrochloric acid (HCl) was generated by dilution of 37% HCl obtained from LOBA Chemie with distilled water. Additionally, the corrosive solution's concentration is titrated using the NaOH solution.

All the experiments were conducted in a 1 M HCl solution, both in the absence and in the presence of varying concentrations (10^{-2}, 10^{-3}, 10^{-4}, 10^{-5} M) of the organic inhibitor «PPMQ». Prior to every test, the carbon steel samples were subjected to several treatments. Initially, the specimens were polished using abrasive paper of different grades, starting from 180 grade and progressing to 2000 grade. This step likely aimed to smoothen and refine the surface of the specimens. After polishing, the specimens underwent a wash with distilled water in order to remove any residues from the polishing process. They were then degreased using acetone. Finally, the specimens were air-dried. These treatments were performed to ensure that the surface of the specimens was chemically active, free from contaminants, and ready for the subsequent experiments.

2.2. Inhibitor

2.2.1. Synthesis and characterization of PPMQ

A combination of techniques was used to characterize and identify this compound. The products used in this study were acquired from Sigma-Aldrich. Additionally, the structure of the synthesized molecule was ascertained using NMR spectroscopy, specifically ^{1}H and ^{13}C

NMR served with an electro-thermal melting point apparatus IA 9200 that operates automatically with the aid of capillary tubes to assess its purity and identity by measuring its melting points. Nuclear Magnetic Resonance spectra were recorded at 300 MHz using a Bruker Advanced 300 WB for Me_2 SO-d_6 solutions. Chemical shifts were measured in δppm with tetramethylsilane (TMS) as an internal standard [12].

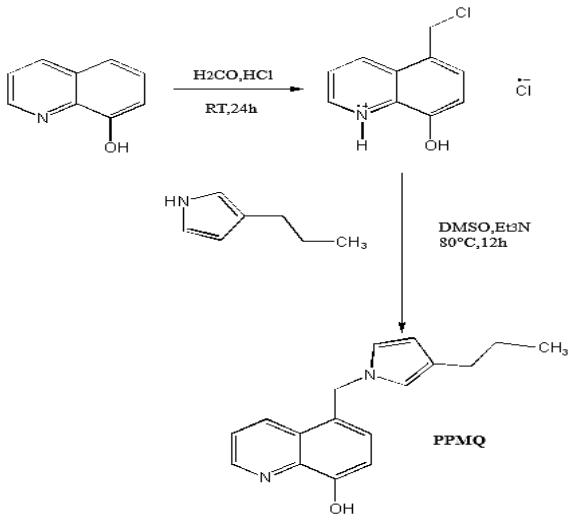

Figure 1. An illustration of the process used to synthesize the compound PPMQ

Figure 1 shows the synthesis of this compound, which involves the reaction of pyrrole derivative condensation with the compound 5-chloromethyl-8-hydroxyquinoline hydrochloride (5-CMHQ) mixed with dimethyl sulfoxide (DMSO) and heated to 80 °C for 12 hours. 8-hydroxyquinoline (HQ) was transformed into the chemical 5-CMHQ using a process that was described in a previous work [13].

For the corrosion test, the compound PPMQ was first dissolved in DMSO and then added to the 1 M HCl corrosive medium at different concentrations.

The characterization of the obtained PPMQ (5-((3-propyl-1H-pyrrol-1-yl) methyl) quinolin-8-ol) is:

Yield 60%, M_p 181–183 °C, R_f 0.41 (n- hexane/dichloromethane: 5/5 (v/v)). IR 1521.68 (C=C), 3335.97 (OH), 2902.93 (CH3), 1429.42 (C-H). ^{1}H δppm 4.35 (s, 2 H, C$\underline{H}_{2\text{the slope between the two functions}}$), 4.34 (s, 1 H, O$\underline{H}$), 2.73 (s, 3 H, C$\underline{H}_{3\text{carbon chain}}$), 2.89 (t, 2 H, C$\underline{H}_{2\text{carbon chain}}$), 3.00 (d, 2 H, C$\underline{H}_{2\text{carbon chain}}$), 7.34–7.57–7.63–8.07–8.09 (m, 5 H, Ar$\underline{H}_{\text{quinoline}}$), 4.37–7.32–7.33 (m, 3 H, C$\underline{H}_{\text{pyrrole}}$). 13C δppm 61.24 (C$\underline{H}_{2\text{ the slope between the two functions}}$), 160.63 (C-OH), 68.90–125.48–126.20–126.84 (C-function Pyrrole), 122.67–127.70–128.64–131.18–132.79–136.70–142.10–157.39 (C-function quinoline). Elemental Analysis ($C_{17}H_{18}N_2O$): Cal. C (%) 76.66; H (%), 6.81, N (%) 10.52, Obt. C (%) 77.00; H (%) 6.79, N (%) 10.24 [12].

2.3. Electrochemical measurements

The OrigaSat 100 electrochemical workstation, provided by the Origa Master 5 software, was equipped with a traditional three-electrode device for use in all corrosion research. The device consisted of a rectangular carbon steel working electrode, a platinum auxiliary electrode, and a reference electrode made of saturated calomel. A polished working electrode with a 0.81cm² exposed region was employed for electrochemical experiments.

Before conducting the electrochemical experiment, for around 30 min, the working electrode was submerged in the sample solution to allow the open circuit potential (OCP) to stabilize. The potentiodynamic polarization curves were measured at a scan rate of 1 mV/s within the potential range of -750 to -100 mV. The impedance data obtained from Nyquist plots were fitted into an equivalent circuit [14].

Using the charge transfer resistance, carbon steel's inhibiting efficiency is determined by [14, 15]:

$$IE(\%) = \frac{Rct - R°ct}{Rct} \times 100 \qquad (1)$$

where the transfer resistance without PPMQ is denoted as R_{ct}, while the transfer resistance with PPMQ is denoted as $R°_{ct}$.

2.4. Thermodynamic parameters

The process of the inhibitor's adsorption on the metal surface was examined using the thermodynamic parameters of the accurate isothermal adsorption model. A variety of adsorption isothermal models, including Langmuir, Temkin, Frumkin, and Freundlich, were created utilizing EIS data to provide more details about the PPMQ adsorption process on the carbon steel surface in 1 M HCl solution at 293-323 K. The best suitable isotherm was selected for the study of thermodynamic parameters related to the inhibiting behavior of the inhibitor.

2.5. Scanning electron microscopic (SEM) measurement

SEM is a powerful technique used for characterizing the surface morphology and microstructure of metal materials, providing high resolution images [16]. This approach involves directing an electron beam toward a sample, resulting in the generation of secondary electrons by surface interaction. These electrons are then gathered to generate a high-quality image [17].

The Zeiss Leo 1550 scanning electron microscope (SEM) was used to analyze the surface condition of the carbon steel (CS) material. The surface microstructure of samples made of carbon steel has been examined through measurements with dimensions of 0.81 cm^2. This examination was conducted in both the absence and presence of an optimized concentration of

10^{-2} M PPMQ in 1 M HCl for 24 hours. SEM micrographs of steel specimens submerged in 1 M HCl solution, both with and without PPMQ, were recorded.

3. RESULTS AND DISCUSSION

3.1. Concentration effect

3.1.1. Potentiodynamic Tafel polarization measurements

Polarization measurements were utilized to analyze the impact of PPMQ concentration on the corrosion behavior of a carbon steel electrode in a 1 M hydrochloric acid solution. The electrochemical Tafel polarization curves for carbon steel at 298-323 K with and without the addition of various amounts of PPMQ are depicted in Figure 2.

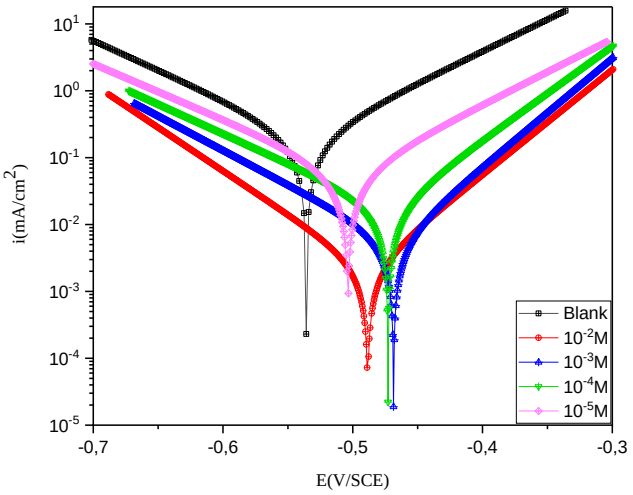

Figure 2. Curves of potentiodynamic polarization for carbon steel in 1 M HCl in the presence and absence of different PPMQ concentrations

Table 1 contains the parameters for extrapolation as well as the values for inhibition efficiency. The graph of current versus potential was established at the specified potential range in frequency between 1 kHz and 100 mHz using a sine wave voltage of 5 mV. The corrosion parameters are provided in Table 1 as corrosion potential (E_{corr}), corrosion current density (i_{corr}), Tafel cathodic slope (β_c), Tafel anodic slope (β_a), and inhibition efficiency (IE) of PPMQ in protecting carbon steel against corrosion in 1M HCl that is calculated using the following expression (2).

The inhibition efficiency IE (%) was determined using corrosion current density in the equation shown below [18-20]:

$$IE(\%) = \frac{i°corr - icorr(inh)}{i°corr} \times 100 \qquad (2)$$

where $i°_{corr}$ and i_{corr} (inh) are the corrosion current densities, determined by extrapolating the cathodic and anodic lines of Tafel after immersing in an acidic solution with or without the inhibitor.

Table 1. Parameters of potentiodynamic polarization for carbon steel in 1 M HCl at different concentrations of PPMQ at 293 K

Concentration (M)	**E_{corr} (mV /SCE)**	**i_{corr} (mA/cm^2)**	**β_a (mV/dec)**	**β_c (mV/dec)**	**IE (%)**
Blank	-535.83	0.198	105.1	-112.9	///
10^{-5}	-503.78	0.059	101.6	-120.2	70.20
10^{-4}	-472.83	0.017	71.1	-113	91.41
10^{-3}	-468.55	0.006	61.6	-97.2	96.97
10^{-2}	-488.51	0.002	63.7	-77	98.99

A preliminary analysis of the graphs in Figure 2 demonstrates that the corrosion potential is enhanced as the inhibitor concentration does. The two partial anode and cathode currents are remarkably diminished with the addition of the inhibitor to the solution.

The potential shift reveals that PPMQ forms a protective layer that prevents the dissolution of carbon steel without altering the reaction process [21].

According to Table 1, the inclusion of PPMQ prevents acid attack on carbon steel. Furthermore, when its concentration increases, anodic and cathodic current densities drop, demonstrating that the derivative of the quinoline compound operates as a mixed-type inhibitor. This shows a decrease in the rate of corrosion as the adsorbed inhibitor particles on the metal surface obstruct charge flow to the electrode [22].

The addition of the PPMQ compound affects the cathodic Tafel slopes (βc). In other words, the change in βc suggests a variation in the cathodic hydrogen evolution mechanism. This modification indicates that this inhibitor has a strong inhibitory effect on the corrosion process of carbon steel [23,24]. Additionally, research showed that as concentrations of the derivative of the quinoline chemical increased, the inhibitory efficiency improved. The maximum inhibition efficiency achieved is reported as 98.99% at a concentration of 10^{-2} M of PPMQ. This suggests that at this concentration, the compound is highly effective at inhibiting corrosion. Moreover, the compound exhibits both cathodic and anodic inhibition mechanisms. This means that it acts by interfering with one and the other the reduction (cathodic) and oxidation (anodic) reactions involved in the process of corrosion. The compound achieves this by adhering to the carbon steel's surface, effectively limiting active sites where corrosion reactions typically occur [24]. Also, E_{corr} values do not exhibit significant variation when the derivative of the quinoline compound is added. This suggests that the introduction of the

compound does not noticeably alter the corrosion process of carbon steel [25,26]. In addition, the variation in E_{corr} values is less than ±85mV when PPMQ is present. This range of variation suggests that PPMQ performs as a mixed-type inhibitor [27].

3.1.2. Electrochemical impedance spectroscopy (EIS) study

Using EIS, the behavior of carbon steel corrosion in an acidic solution (1.0 M HCl) with the compound (PPMQ) was examined by EIS at 293 K, after being submerged for 30 minutes at the corrosion potential.

Nyquist curves in the presence and absence of various inhibitor concentrations based on data from electrochemical impedance experiments are illustrated in Figure 3. The impedance spectra mainly display depressed semicircles, which symbolize a general charge transfer-controlled corrosion reaction mechanism [28]. The loops grow to their largest diameter at the highest concentration. The impedance parameters derived from this study, such as R_s, R_{ct}, Q_{dl}, n, $C_{dl,}$ and inhibition efficiency IE(%), are generated and listed in Table 2 after being fitted to the EIS data using the equivalent circuit of Figure 3 [29]. It can be seen that as the concentration of PPMQ rises, inhibition efficiency enhances to a value of 95.93% at 10^{-2} M. It has also been shown that the R_{ct} values increase along with the addition of inhibitor concentration. This implies that greater adsorption of the adsorbent on the metal surface is caused by higher resistance to charge transfer R_{ct} [30]. Moreover, as PPMQ concentration increased, the values of double-layer capacitance C_{dl} diminished. Which is related to the adsorption of PPMQ molecules on the CS surface that have a greater affinity for the water molecules [31]. This results in a decrease in the local dielectric constant and/or an increase in the thickness of the electrical double layer [32].

Table 2. Electrochemical parameters determined from EIS plots for CS in 1.0 M HCl without and with PPMQ at different concentrations

Conc of inh (M)	**R_s(ohm.cm^2)**	**R_{ct}(ohm.cm^2)**	**C_{dl}(µF.cm^{-2})**	**Q_{dl}(µF.S^n.cm^{-2})**	**n**	**IE (%)**
Blank	0.9951	110.9	131	217.3	0.8811	----
10^{-5}	7.852	318.3	41.19	60.53	0.9112	65.16
10^{-4}	0.3444	974.1	42.76	66.47	0.8612	88.62
10^{-3}	6.781	1764	27.86	38.81	0.89	93.71
10^{-2}	1.254	2726	41.45	50.97	0.9052	95.93

The C_{dl} values were calculated by the equation below [33]:

$$\mathrm{Cdl} = \frac{\varepsilon\varepsilon_0 A}{\delta} \qquad (3)$$

Here, ε represents the dielectric constant of the protective film, ε_0 represents the free space permittivity, δ is the thickness of the protective film, and A is the electrode's surface area.

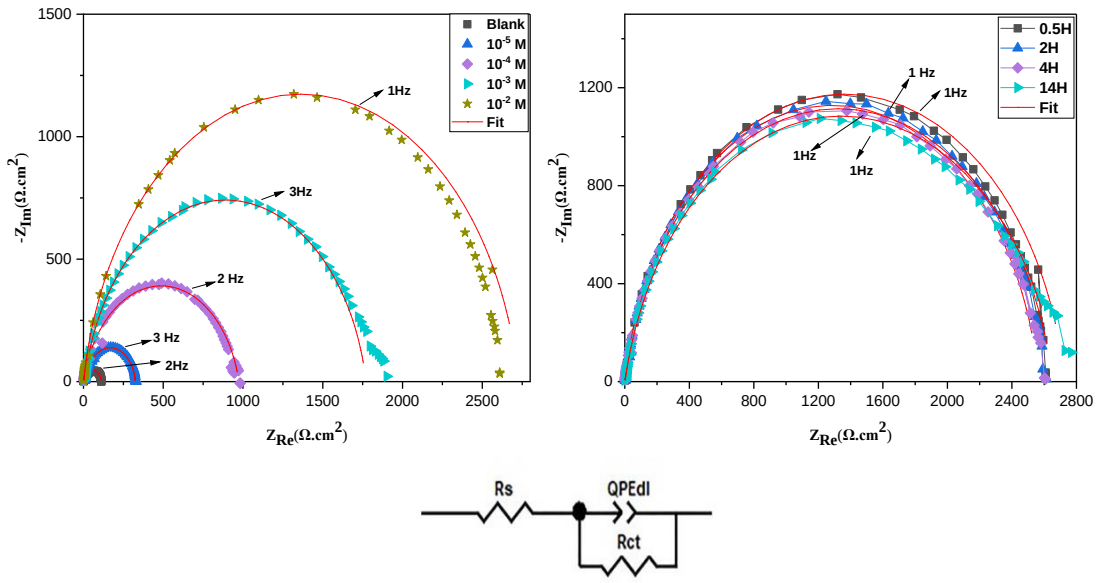

Figure 3. Impedance spectra for CS in 1.0 M HCl with the absence and the presence of different concentrations of PPMQ and at various immersion times 0.5, 2, 4, 14 H at 293 K and the Electrical Equivalent circuit for carbon steel/HCl interface [27]

We assembled in Table 3 [34,35] a comparative analysis of PPMQ and some selected compounds from the same family to compare their corrosion inhibition performance in acidic solution 1 M HCl, by EIS at 298 K after a half-hour of immersion at the corrosion potential. It is noticed that PPMQ exhibits potent inhibitory efficiency, comparable to other compounds. Each inhibition efficiency is related to the molecule structure of each inhibitor.

3.2. Immersion time effect

To learn more about a carbon steel electrode's corrosion behavior in corrosive environments. With the open circuit potential (OCP) held constant, impedance measurements in 1 M HCl solution were carried out in both the presence and absence of PPMQ at various immersion times. Figure 3 depicts the Nyquist curves for the carbon steel specimen in a 1 M HCl solution containing 10^{-2} M PPMQ at various immersion times as measured at open circuit potential.

To assess the stability of the inhibitor's adsorption rate and to understand if the inhibitor molecules maintain their effectiveness in inhibiting the corrosion process over extended periods in the aggressive acidic environment of 1 M hydrochloric acid.

The investigations of immersion time were performed in different time intervals 0.5, 2,4, and 14H.

Table 3. Percentage inhibition efficiency for other organic inhibitors in 1 M HCl

Compound/ structure	Highest inhibition efficiency	Metal	Reference
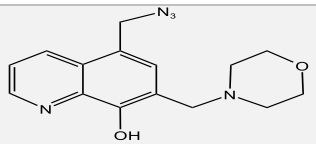 **5-Azidomethyl-7-morpholinomethyl-8-hydroxyquinoline**	90% at 10^{-3} M	Mild steel	[32]
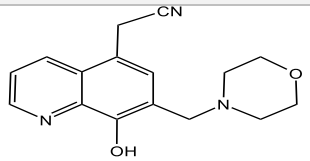 **5-Cyanomethyl-7-morpholinomethyl-8-hydroxyquinoline**	89% at 10^{-3} M	Mild steel	[32]
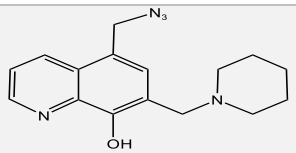 **5-Cyanomethyl-7-piperidinomethyl-8-hydroxyquinoline**	88% at 10^{-3} M	Mild steel	[32]
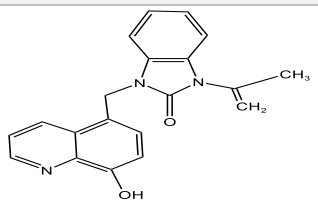 **1-((8-hydroxyquinolin-5-yl)methyl)−3-(prop-1-en-2-yl)−1H-benzimidazol-2(3H)-one**	94.5% at 10^{-3} M	Carbon steel	[33]
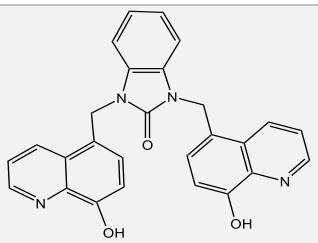 **1,3-bis((8-hydroxyquinolin-5-yl)methyl)−1H-benzimidazol-2(3H)-one**	93.6% at 10^{-3} M	Carbon steel	[33]
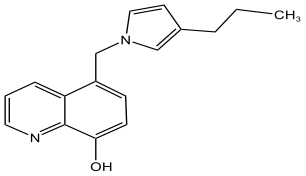 **[5-((3-propyl-1H-pyrrol-1-yl) methyl) quinolin-8-ol]**	95.9% at 10^{-2} M	Carbon steel	This work

The results of the EIS experiment for carbon steel immersed in 1 M HCl with an optimal concentration of 10^{-2} M of the inhibitor are shown in Figure 3 and Table 4. We can deduce that the inhibition efficiency remained almost stable along with exposure time. The highest value was attended at 14H of immersion. During this time interval of CS in 10^{-2} M solution, the highest value of inhibition efficiency came out to be 95.94% for PPMQ. This inhibitor showed higher inhibition efficiency as soon as it was immersed at 0.5H. The greatest amount of inhibitor molecules isolating the metal's surface from the corrosive solution led to the quick adsorption of the compound molecules onto the surface of carbon steel, which is what contributed to this result [36].

Table 4. Electrochemical parameters and anticorrosion efficiency for CS electrode in 1 M HCl electrolyte with 10^{-2} M PPMQ at diverse immersion times

Immersion time (H)	**R_s (ohm.cm^2)**	**R_{ct} (ohm.cm^2)**	**C_{dl} (µF.cm^{-2})**	**Q_{dl} (µF.S^n.cm^{-2})**	**n**	**IE (%)**
0.5	1.254	2726	41.45	50.97	0.9052	95.93
2	1.396	2630	58.05	66.37	0.9287	95.78
4	0.4466	2682	43.47	53.83	0.9005	95.86
14	1.277	2730	48.72	69.12	0.8266	95.94

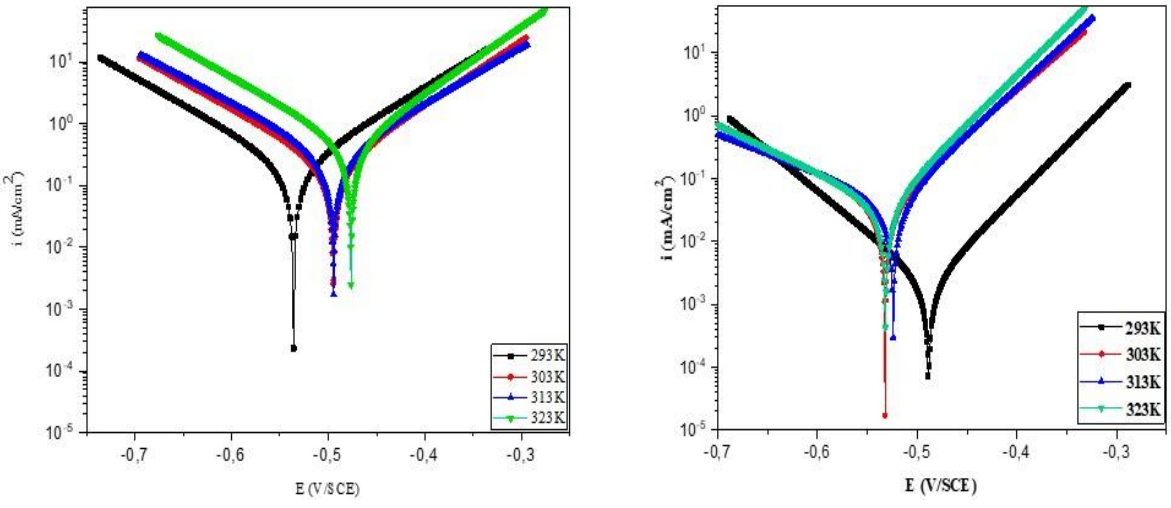

Figure 4. Potentiodynamic polarization plots for carbon steel in 1.0 M HCl in (a) blank solution and (b) adding 10^{-2} M of PPMQ at various temperatures

3.3. Temperature effect

The impact of temperature on the inhibition process is a crucial factor to consider in corrosion research and inhibitor development. In other words, the inhibition efficiency of corrosion inhibitors is significantly influenced by temperature [32]. In the temperature range of (293, 303, 313, and 323 K), the potentiodynamic polarization curves for carbon steel in 1 M HCl in the absence and presence of 10^{-2} M of PPMQ have been investigated. Figure 4 demonstrates the outcomes, accordingly. These curves appeared to display Tafel regions indicating that this electrochemical corrosion process follows Tafel kinetics. Also, we can deduce that increasing temperature causes anodic and cathodic branches to increase.

Table 5. Electrochemical parameters of carbon steel in 1.0 M HCl without and with 10^{-2} M of PPMQ at different temperatures

	T (K)	**i_{corr}(μA/cm^2)**	**E_{corr}(mV/SCE)**	**β_a(mV/dec)**	**β_c (mV/dec)**	**IE (%)**
Blank solution	293	198	-535.83	105.1	-112.9	---
	303	213	-494.72	96.8	-115.5	---
	313	295	-494.55	110.2	-121.5	---
	323	471	-476.52	93.1	-114.1	---
10^{-2} M PPMQ	293	2	-488.51	63.7	-77	98.99
	303	38	-532.2	72.8	-131.7	82.16
	313	42	-524.1	68.2	-164.1	85.76
	323	38	-531.7	64.1	-132.3	91.93

Table 5 lists the electrochemical parameters that were calculated from Tafel plots. It is observed that the rate of corrosion increased along with an increase in temperature. Additionally, it can be noted that at 303 K, the investigated compound's inhibition efficiency value slightly declines, then increases to achieve 91.93 % at 323 K. This shows a key feature of the physical adsorption of this temperature-dependent inhibitor [37].

The decrease in inhibition efficiency of PPMQ at 303 K showed the instability of this compound when it was subjected to higher temperatures due to its desorption from the carbon steel surface implying an exothermic process of PPMQ adsorption [38]. While the enhanced effectiveness of PPMQ inhibition at 313 K and 323 K is indicative of a chemical adsorption mechanism that was successfully boosted with higher temperatures [39]. Therefore, PPMQ exhibits good performance on the CS surface in the HCl medium.

3.4. Adsorption isotherm and thermodynamic parameters

Several adsorption isotherms were investigated to better understand how this inhibitor adheres to the surface of the metal. The adsorption isotherm of Langmuir was found to give

the best fit with (strong correlation with $R^2 \approx 1$) obtained for the plot of C_{inh}/θ vs. C_{inh} presented in Figure 5 following the equation below [40].

$$\frac{Cinh}{\theta} = \frac{1}{Kads} + C\,inh \qquad (4)$$

Here, C_{inh} stands for the concentration, K_{ads} is the adsorption equilibrium constant and θ is the surface coverage.

Using equation (5), the values of Gibb's free adsorption energy ($\Delta G°_{ads}$) were determined [41]:

$$\Delta G°ads = -RT \ln (55.5K) \qquad (5)$$

where R is the universal gas constant, T is the absolute temperature and the value of 55.5 is the approximate concentration (mol L^{-1}) of water in the solution.

The intercept value of the line served as the source for the K_{ads} values. Negative values of Gibb's free adsorption indicated that the adsorption process was spontaneous. The K_{ads} value of PPMQ is 1.12×10^5 M^{-1} which indicates a great interaction metal-inhibitor [41]. The $\Delta G°_{ads}$ value obtained is -38.76 kJ/mol, which is found to be greater than -20 KJ/mol and lower than -40 KJ/mol proposing a spontaneous adsorption indicated by the chemisorption and the physisorption mechanisms of inhibitory species on a carbon steel surface [42,43]. Therefore, we can deduce that the strong adsorption of water molecules on the carbon steel (CS) surface occurs primarily through physical forces, and then as the corrosion inhibitor PPMQ molecules are introduced into the acidic media, they can displace water molecules from their sites due to stronger binding forces and specific chemical interactions between the metallic area and the adsorbate particles [44].

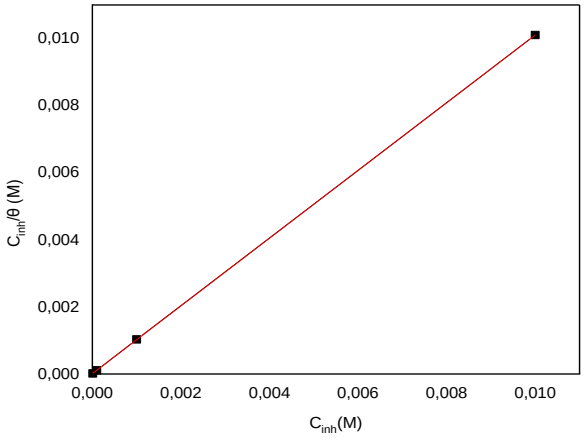

Figure 5. Graph of the Langmuir adsorption isotherm of PPMQ on the carbon steel surface at 293 K

Calculating the kinetic parameters of the activation, such as the energy of activation (E_a), enthalpy of activation (ΔH_a), and entropy of activation (ΔS_a), is crucial in understanding the corrosion process and the inhibition efficiency of corrosion inhibitors. These parameters

provide insights into the energy barrier that must be overcome for the corrosion reactions to occur and the nature of the corrosion inhibition process. Modeling the corrosion current density (i_{corr}) with temperature can often be achieved through an Arrhenius-type process, as shown in the equation (6) [24].

$$Ln\ (icorr) = LnA - \frac{\boldsymbol{Ea}}{RT} \qquad (6)$$

Where E_a is the corrosion process apparent activation energy, R is the universal gas constant, A is the pre-exponential constant of Arrhenius, and T stands for the absolute temperature.

The graph of Ln i_{corr} vs 1000/T without and with 10^{-2} M PPMQ gave a straight-line plot as illustrated in Figure 6 with a slope permitting the determination of E_a. It is shown that the rise in temperature for the blank solution makes it noticeable that the corrosion rate increases indicating that the corrosion process is accelerated significantly as the temperature increases. Whereas, in the presence of the corrosion inhibitor PPMQ, the corrosion rate is slightly increased at explored temperatures. The activation energy (E_a) value in the presence of PPMQ obtained is about 49.73 kJ/mol, which is significantly higher compared to the inhibitor-free acid solution (22.8 kJ/mol). This strongly suggests that certain inhibitor molecules have physically adsorbed onto the surface of CS [45]. Moreover, the rise in the E_a with the presence of PPMQ consequences in the reduction of i_{corr} of the CS, hence an increase in the anticorrosion efficiency [46]. Furthermore, according to Eddy et al, E_a values below 80 kJ mol-1 indicate a physical action, but E_a values above 80 kJ mol-1 indicate a chemical action. Therefore, we can deduce that the interaction between the PPMQ molecules and the CS area was controlled by the chemical adsorption [47].

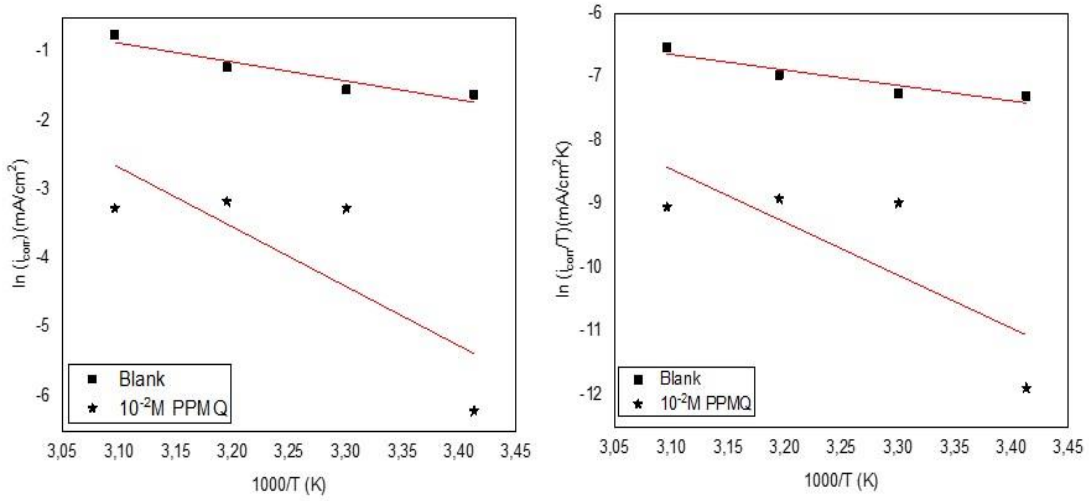

(a) **(b)**

Figure 6. (a) Arrhenius plots (b) Transition state plots of carbon steel in 1.0 M HCl without and with 10^{-2} M of PPMQ

The Arrhenius equation's alternate formulation was used to calculate additional kinetic parameters using equation (7) [24]:

$$Ln\left(\frac{icorr}{T}\right) = Ln\left(\frac{R}{Nh} + \frac{\Delta Sa}{R}\right) - \frac{\Delta Ha}{R}\frac{1}{T} \quad (7)$$

where T, R N, and h are the absolute temperature, the gas molar constant, the Avogadro's and the Planck's constant, correspondingly.

The Ln (i_{corr}/T) function (1000/T) variation is depicted in Figure 6 as a straight line with a slope of ($-\Delta H_a/R$) and the intersection with the y-axis of [Ln(R/N h) + ($\Delta S_a/R$)].

The ΔH_a value for the dissolution reaction of carbon steel in 1 M HCl in the presence of PPMQ obtained is 69.26 kJ/mol which is found to be greater compared to the one in the blank solution (20.25 kJ/mol). Accordingly, the dissolution of carbon steel occurs endothermically, as seen by the positive sign of the enthalpy of activation (H_a). In other words, the positive ΔH_a suggests that breaking the bonds at the metal surface during the initial stages of the corrosion process requires energy input. As the temperature increases, more energy is available, facilitating this bond-breaking process and leading to a greater corrosion rate [24]. In the presence of the inhibitor, the activation entropy (ΔS_a) has a value of -53.11 J mol^{-1} K^{-1}. In contrast, when it is absent, it is -190.03 J mol^{-1} K^{-1}. ΔS_a readings are clearly more likely to be negative than for the acid electrolyte in the absence of the inhibitor. ΔS_a values enhanced in the presence of the studied inhibitor, indicating the instability of the formed layer inhibitory due to the presence of H_2O molecules that substituted with the inhibitor molecules in the aqueous phase on the electrode surface [48, 32].

3.5. SEM analysis results

Carbon steel's surface examination has been studied using SEM. The microscopic images of the carbon steel surface obtained before and after it was submerged in 1.0 M HCl for 24 hours at 293 K in the blank solution and with the addition of 10^{-2} M PPMQ are shown in Figure 7.

The polished carbon steel Figure 7(a) exhibits a smooth surface, but once immersed in the 1 M HCl solution exhibited the presence of pores filled with micro-cracks as shown in Figure 7(b), further confirming the occurrence of pitting corrosion. However, the presence of inhibitor Figure 7(c), contributed to the amelioration of the smoothness of the CS surface. Consequently, it follows that the inhibitor PPMQ was effective in reducing the deterioration of carbon steel. Moreover, the metal's surface was covered with a protective layer of the inhibitor that may shield the reactive center and successfully stop corrosive media from coming into touch with the metal matrix, delaying the carbon steel's corrosion, and confirming that PPMQ is an effective inhibitor for CS in acidic medium [49,50].

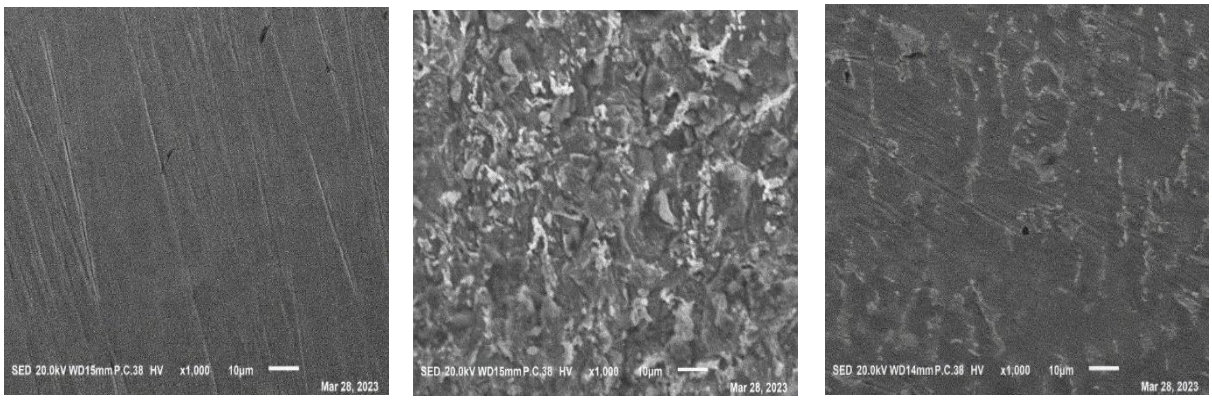

(a) **(b)** **(c)**

Figure 7. SEM micrographs of carbon steel surfaces: (a) with polishing, (b) with 24 hours of immersion in 1M HCl, and (c) with 24 hours of immersion in 1 M HCl with 10^{-2} M of PPMQ inhibitor.

3.6. Inhibition mechanism

In order to elucidate the inhibitory mechanism of PPMQ in controlling carbon steel corrosion in acidic solutions, it is necessary to understand the electrical charge carried by steel in such solutions.

For this purpose, the investigation of the total charge (E_{total}) on a metal surface in aqueous solutions can be conducted using the equation: $E_{total} = E_{corr} - E_q = 0$.

The optimal value of equilibrium zero charge corrosion potential E_q=0 of carbon steel in 1 M HCl should be -485 mV [51]. This indicates that carbon steel was positively charged in acidic environments with and without inhibitors. As a result, direct adsorption of protonated PPMQ molecules on carbon steel would be complicated.

This information suggested that in acidic conditions, the carbon steel surface was first adsorbed with chloride ions, which produced excess negative charges near the surface [52,53]. Subsequently, due to electrostatic forces, a bond was created between carbon steel forces and inhibitor molecules. The change in Ecorr values in the cathodic direction (Table 1), was another indication of an increase in negative charges, which confirmed our interpretation.

Furthermore, lone pair electrons (O and N) of the PPMQ molecule and the d orbital electrons of iron and π electrons might establish a chemical connection that would allow PPMQ to interact with iron.

Therefore, it is possible to conclude that the adsorption of inhibitor molecules at the mild steel surface's active sites resulted in a delayed rate of corrosion in acidic solutions. Moreover, as the inhibitor concentration increased, the rates of corrosion further decreased, confirming that corrosion inhibition was established only by having PPMQ molecules adsorb on the metal surface in HCl [54].

4. CONCLUSION

The corrosion protection performance of PPMQ as an organic inhibitor has been evaluated in this work, utilizing surface analysis and electrochemical tests. PPMQ is found to be an effective corrosion inhibitor for carbon steel in 1 M HCl. The inhibition efficiency was enhanced with the increase in concentration attending a higher value of 95.93% at a concentration of 10^{-2} M at 293 K and remained almost constant with exposure time. This inhibitor showed great resistance to higher temperatures. The inhibitor adsorption, in accordance with the SEM data, results in the formation of a barrier of protection on the CS surface. The adsorption process adheres to Langmuir's adsorption isotherm model, which implies both physisorption and chemisorption and an endothermic process.

Declarations of interest

The authors declare no conflict of interest in this reported work.

REFERENCES

[1] K. Chkirate, K. Azgaou, H. Elmsellem, and et al., J. Molecular Liq. 321 (2021) 114750.
[2] K.R. Singh, D. Ansari, S. Chauhan, M.A. Quraishi, H. Lgaz, and I.M. Chung, J. Colloid Interface Sci. 560 (2019) 225.
[3] B.M. Praveen, B.M. Prasanna, N.M. Mallikarjuna, M.R. Jagadeesh, N. Hebbar, and D. Rashmi, Heliyon 7 (2021) e06090.
[4] Y. Zhang, Y. Pan, P. Li, X. Zeng, B. Guo, J. Pan, L. Hou, and X. Yin, Colloids and Surfaces A 623 (2021) 126717.
[5] S.V. Lamaka, M.L. Zheludkevich, K.A. Yasakau, M.F. Montemor, and M.G.S. Ferreira, Electrochim. Acta 52 (2007) 7231.
[6] H. Gao, Q. Li, Y. Dai, F. Luo, and H.X. Zhang, Corr. Sci. 52 (2010) 1603.
[7] M. Abdel-All, Z. Ahmed, and M. Hassan, J. Appl. Electrochem. 22 (1992) 1104.
[8] A.A. Watson, G.W.J. Fleet, N. Asano, R.J. Molyneux, R.J. Nash, Phytochemistry 56 (2001) 265.
[9] G.J. Atwell, B.C. Baguley, and W.A. Denny, J. Med. Chem. 32 (1989) 396.
[10] Y. Xia, Z.Y. Yang, P. Xia, K.F. Bastow, Y. Tachibani, S.C. Kuo, E. Hamel, T. Hackl, and K.H. Lee, J. Med. Chem. 41 (1998) 1155.
[11] A.M. El-Agrody, E. Khattab, A. M. Fouda, and A.M. Al-Ghamdi, Medicinal Chem. Res. 12 (2012) 4200.
[12] Y. Lakhrissi, M. Rbaa, B. Tuzun, A. Hichar, E.H. Anouar, K. Ounine, F. Almalki, T. Ben Hadda, A. Zarrouk, and B. Lakhrissi, J. Molecular Structure 1259 (2022) 132683.
[13] M. Rbaa, and B. Lakhrissi, Surf. Interfaces 15 (2019) 43.
[14] Y. Elkhotfi, I. Forsal, and E.M. Rakib, Portugaliae Electrochim. Acta 36 (2018) 77.

[15] C. Belmejdoub, N. Errahmany, H. Hailou, K. Benbouya, M. Chahboune, I. Forsal, S. Lahmady, Y. Ramli, and R. Touir, Mor. J. Chem. 12 (2024) 970.
[16] H.S. Samuel, E.E. Etim, U. Nweke-Maraizu, B. Bako, and J.P. Shinggu, J. Appl. Sci. Environ. Manage 27 (2023) 2957.
[17] K.S. Bokati, and C. Dehghanian, J. Environ. Chem. Eng. 6 (2018) 1613.
[18] H. Boubekraoui, I. Forsal, M. Ellaite, K. Benbouya, and H. Hanin, Anal. Bioanal. Electrochem. 13 (2021) 80.
[19] H. Boubekraoui, I. Forsal, H. Ouardi, Y.Elkhotfi, and H. Hanin, Anal. Bioanal. Electrochem. 12 (2020) 828.
[20] S. Lahmady, O. Anor, I. Forsal, H. Hanin, and K. Benbouya, Anal. Bioanal. Electrochem. 14 (2022) 303.
[21] I.B. Obot, N.O. Obi-egbedi, and S. Umoren, Int. J. Electrochem. Sci. 4 (2009) 863.
[22] Y. El Kacimi, M.A. Azaroual, R. Touir, M. Galai, K. Alaoui, M. Sfaira, M. Ebn Touhami, and S. Kaya, Euro-Mediterranean J. Environ. Integr. 2 (2017) 11.
[23] M. El Faydy, N. Dahaief, M. Rbaa, K. Ounine, and B. Lakhrissi, J. Mater. Environ. Sci. 7 (2016) 356.
[24] M. Galai, M. El Faydy, Y. El Kacimi, K. Dahmani, K. Alaoui, R. Touir, B. Lakhrissib, and M. Ebn Touhami, Portugaliae Electrochim. Acta 35 (2017) 233.
[25] C.B. Verma, M.A. Quraish, and E.E. Ebenso., Int. J.Electrochem. Sci., 2013,8, 7401.
[26] Y. Wang, and G.A. Voth, J. Phys. Chem. B 110 (2006) 18601.
[27] S. Bashir, V.Sharma, H. Lgaz, I-M. Chung, A. Singh, and A. Kumar, J. Mol. Liq. (2018) 263.
[28] D.K. Yadav, D. Chauhan, I. Ahamad, and M. Quraishi, RSC Advances 3 (2013) 632.
[29] O. Fergachia, F. Benhiba, M. Rbaa, R. Touir, M. Ouakki, M. Galai, B. Lakhrissi, H. Oudda, and M. Ebn Touhami, Mater. Res. 21 (2018) e20171038.
[30] G.A. Zhang, X.M. Hou, B.S. Hou, H.F. Liu, Journal of Molecular Liquids, 2019, 278,413.
[31] P. Han, C. Chen, W. Li, H. Yu., Y. Xu, L. Ma, and Y. Zheng, J. Colloid and Interface Sci. 516 (2018) 398.
[32] M. Rbaa, M. Galai, M. EL Faydy, Y. El Kacimi, M. Ebn Touhami, A. Zarrouk, and B. Lakhrissi, J. Mater. Environ. Sci. 8 (2017) 3529.
[33] B.M. Praveen, B.M. Prasanna, N.M. Mallikarjuna, M.R. Jagadeesh, N. Hebbar, and D. Rashmi, Heliyon 7 (2021) e06090.
[34] D. Douche, H. Elmsellem, E.H Anouar, L. Guo, B. Hafez, B. Tüzün, A. El Louzi, K. Bougrin, K. Karrouchi, and B. Himmi, J. Molecular Liq. 308 (2020) 113042.
[35] M. El Faydy, M.Rbaa, L. Lakhrissi, B. Lakhrissi, I. Warad, A. Zarrouk, and I.B. Obot, Surfaces and Interfaces 14 (2019) 222.
[36] S. Al-Baghdadi, T.S. Gaaz, A. Al-Adili, A.A. Al-Amiery, and M.S. Takriff, Int. J. Low-Carbon Technol. 16 (2021) 181.

[37] R. Solmaz, G. Kardaş, M. Çulha, B. Yazıcı, and M. Erbil, Electrochim. Acta 53 (2008) 5941.
[38] M.G. Tsoeunyane, M.E. Makhatha, and O.A. Arotiba, Int. J. Corr. (2019) 1.
[39] E.A. Noor, Int. J. Electrochem. Sci. 2 (2007) 996.
[40] H. Elmsellem, T. Harit, A. Aouniti, and F. Malek, Protection of Metals and Physical Chemistry of Surfaces 51 (2015) 873.
[41] I.B. Obot, and N.O. Obi-Egbedi, Corros. Sci. 52 (2010) 657.
[42] P.P. Kumari, S.A. Rao, P. Shetty, Procedia Mater. Sci. 5 (2014) 499.
[43] I. Chakib, H. Elmsellem, N.K. Sebbar, S. Lahmidi, A. Nadeem, E.M. Essassi, Y. Ouzidan, I. Abdel-Rahman, F. Bentiss, and B. Hammouti, J. Mater. Environ. Sci. 7 (2016) 1866.
[44] L.M. Vračar, and D.M. Dražić, Corr. Sci. 44 (2002) 1669.
[45] A. Benabida, M. Galai, M. Cherkaoui, and O. Dagdag, Anal. Bioanal. Electrochem. 8 (2016) 962.
[46] A. Biswas, S. Pal, and G. Udayabhanu, Applied Surface Sci. 353 (2015) 173.
[47] N. Eddy, and E. Ebenso, Pure and Applied Chem. 2 (2008) 46.
[48] M. Pramudita, and M. Nasikin, IOP Conference Series: Mater. Sci. Eng. 796 (2020) 012059.
[49] B. Jiang, W. Sun, J. Cai, S. Chen, and B. Hou, Colloids and Surfaces A: Physicochemical and Engineering Aspects 624 (2021) 126824.
[50] O.O. Ogunleye, A.O. Arinkoola, O.A. Eletta, Y.A. Osho, A.F. Morakinyo, and J.O. Hamed, Heliyon 6 (2020) e03205.
[51] M. Elachouri, M.S. Hajji, S. Kertit, E.M. Essassi, M. Salem, and R. Coudert, Corr. Sci. 37 (1995) 381.
[52] M. Lebrini, M. Lagrenée, H. Vezin, L. Gengembre, and F. Bentiss, Corr. Sci. 47 (2005) 485.
[53] S. Deng, and X. Li, Corr. Sci. 64 (2012) 253.
[54] G. Shahi, C. Bhan Verma, E.E. Ebenso, and M.A. Quraishi, Int. J. Electrochem. Sci. 10 (2015) 1102.